



SCI-328 Symposium

Flight Testing of Unmanned Aerial Systems (UAS)

Segovia, Spain, 12-13 May 2022

Numerical and Experimental Study of a Biomimetic UAV with Grids

Rafael Bardera Mora

Ángel Rodríguez-Sevillano

Estela Barroso Barderas

Juan Carlos Matías García

Javier Muñoz Campillejo

Experimental Aerodynamics

National Institute for Aerospace Technology (INTA)

Torrejón de Ardoz, Madrid

SPAIN



1.0 INTRODUCTION

2.0 NUMERICAL ANALYSIS

3.0 EXPERIMENTAL SET-UP

3.1 Low-Speed Wind Tunnel

3.2 Manufacturing process

3.3 Experimental tests

4.0 RESULTS

5.0 SUMMARY AND CONCLUSIONS

1.0 INTRODUCTION

The National Institute for Aerospace Technology (INTA) is developing Biomimetic Unmanned Aerial Vehicles (UAVs).

Morphing model



Adaptative wing geometry by using Macro Fiber Composite (MFC) actuators.

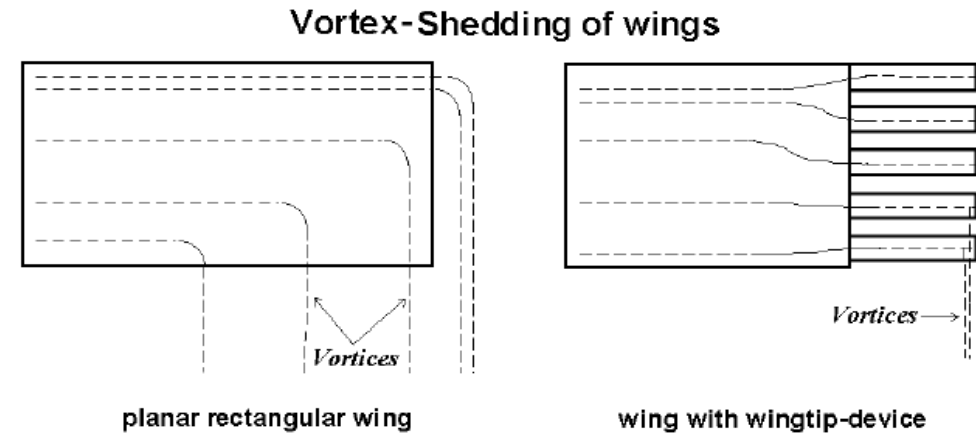
Wing-grid model



Winglets at the tip of the wing to simulate the primary feathers of birds.

1.0 INTRODUCTION

Wing-grid Device: Several grids located at the tip of a wing with gaps between them simulating the **primary** feathers of birds.



Bennett, D. "The Wing Grid: A New Approach to Reducing Induced Drag," 2001

- **Redistributing the large vortices, creating several smaller vortices with smaller intensity.**
- **The loss of energy is reduced.**
- **Wing Grid configuration seems to be a promising mechanism of induced drag reduction.**

1.0 INTRODUCTION

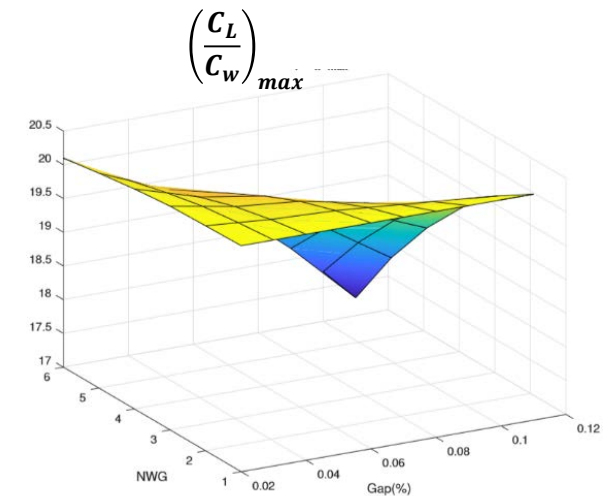
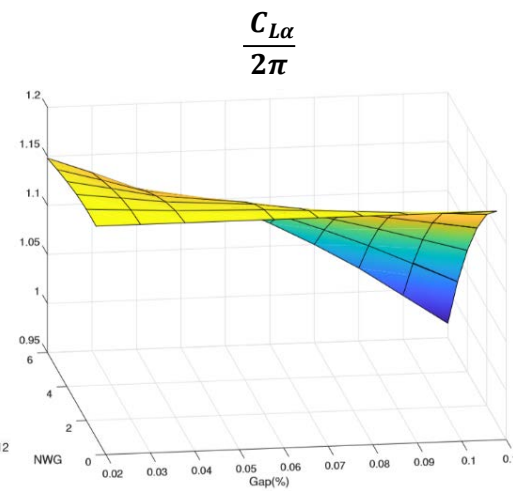
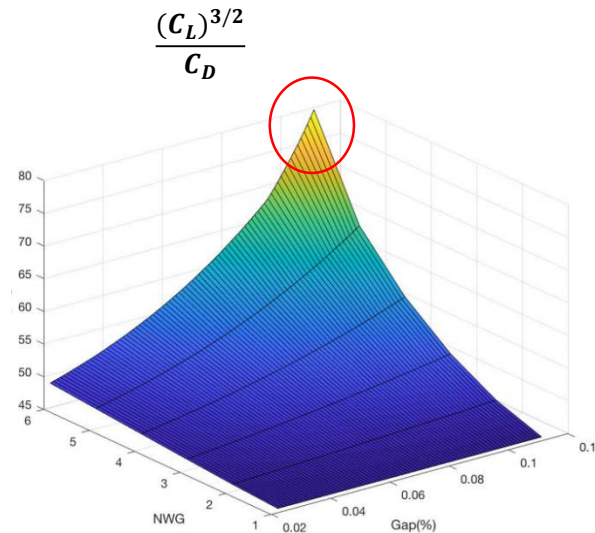
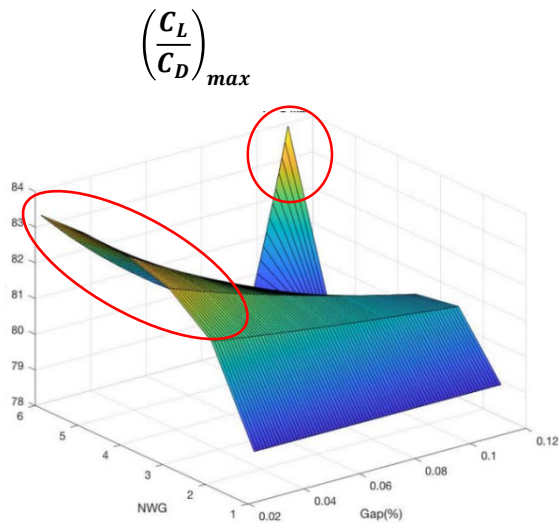
Numerical analysis with Tornado software to optimize

- number of grids (NWG)
- gap between them.

3 grids

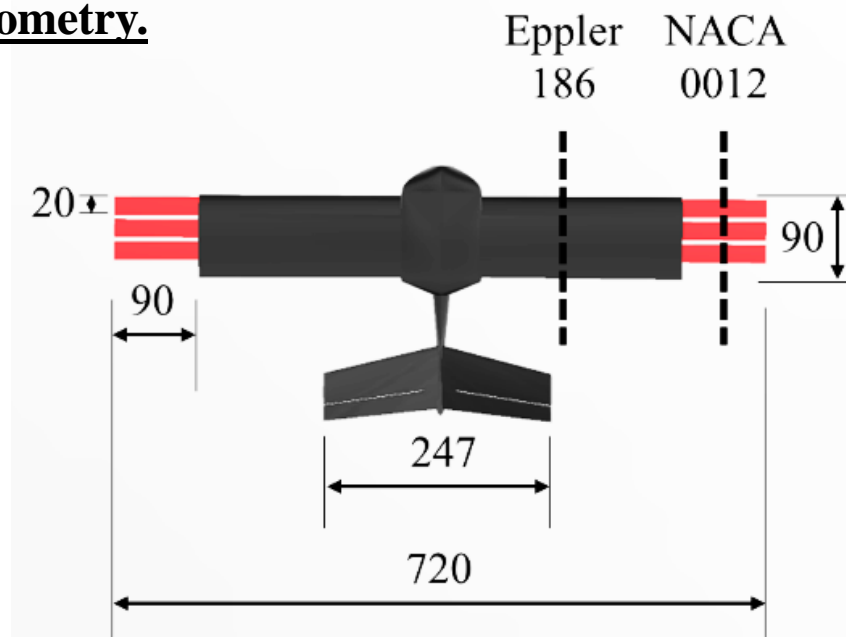


The studied aerodynamics parameters were:

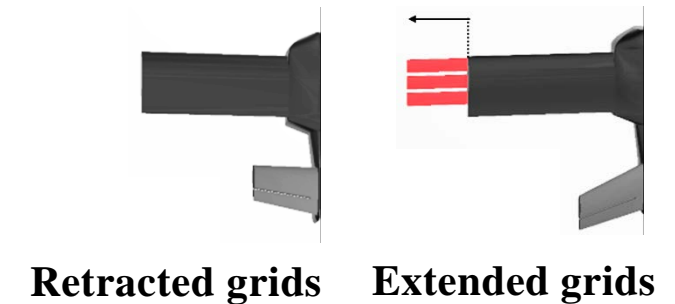


1.0 INTRODUCTION

Geometry.



UAV Configuration	Retracted grids	Extended grids
Aspect Ratio	6	8
Wingspan (m)	0.54	0.72
Chord (m)	0.09	0.09
Wing area (m ²)	0.0486	0.0648



Objectives

1. Aerodynamic efficiency of the UAV with extended and retracted grids.
2. Validation of experimental and numerical data.



1.0 INTRODUCTION

2.0 NUMERICAL ANALYSIS

3.0 EXPERIMENTAL SET-UP

3.1 Low-Speed Wind Tunnel

3.2 Manufacturing process

3.3 Experimental tests

4.0 RESULTS

5.0 SUMMARY AND CONCLUSIONS

2.0 NUMERICAL ANALYSIS

CFD simulations.



Conditions:

- Two UAV configurations:
 - **Retracted grids.**
 - **Extended grids.**
- Half of the model.
- Several angles of attack: from -10° to 25° with a step of 5° .
- Airflow velocity of 16 m/s ($Re = 9.2 \times 10^4$).

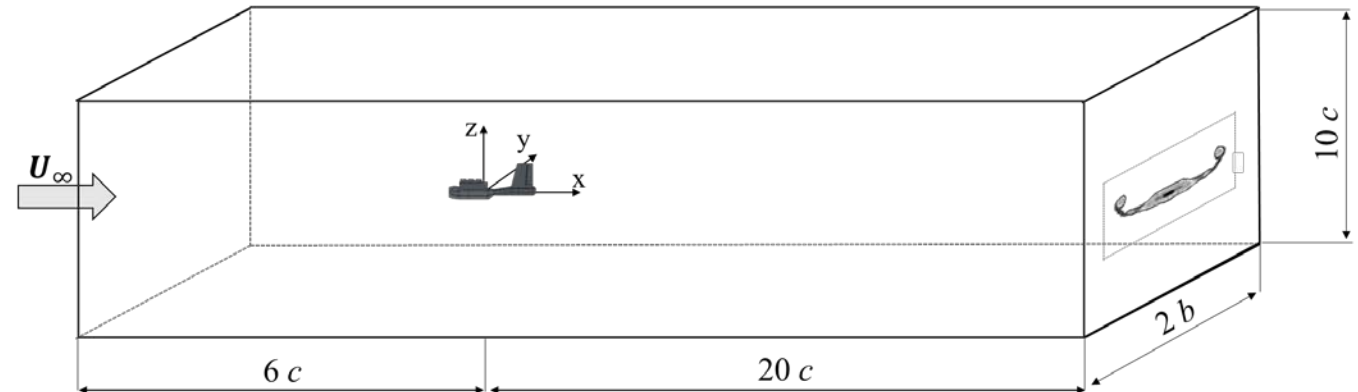
Retracted grids



Extended grids



Computational Flow Domain



2.0 NUMERICAL ANALYSIS

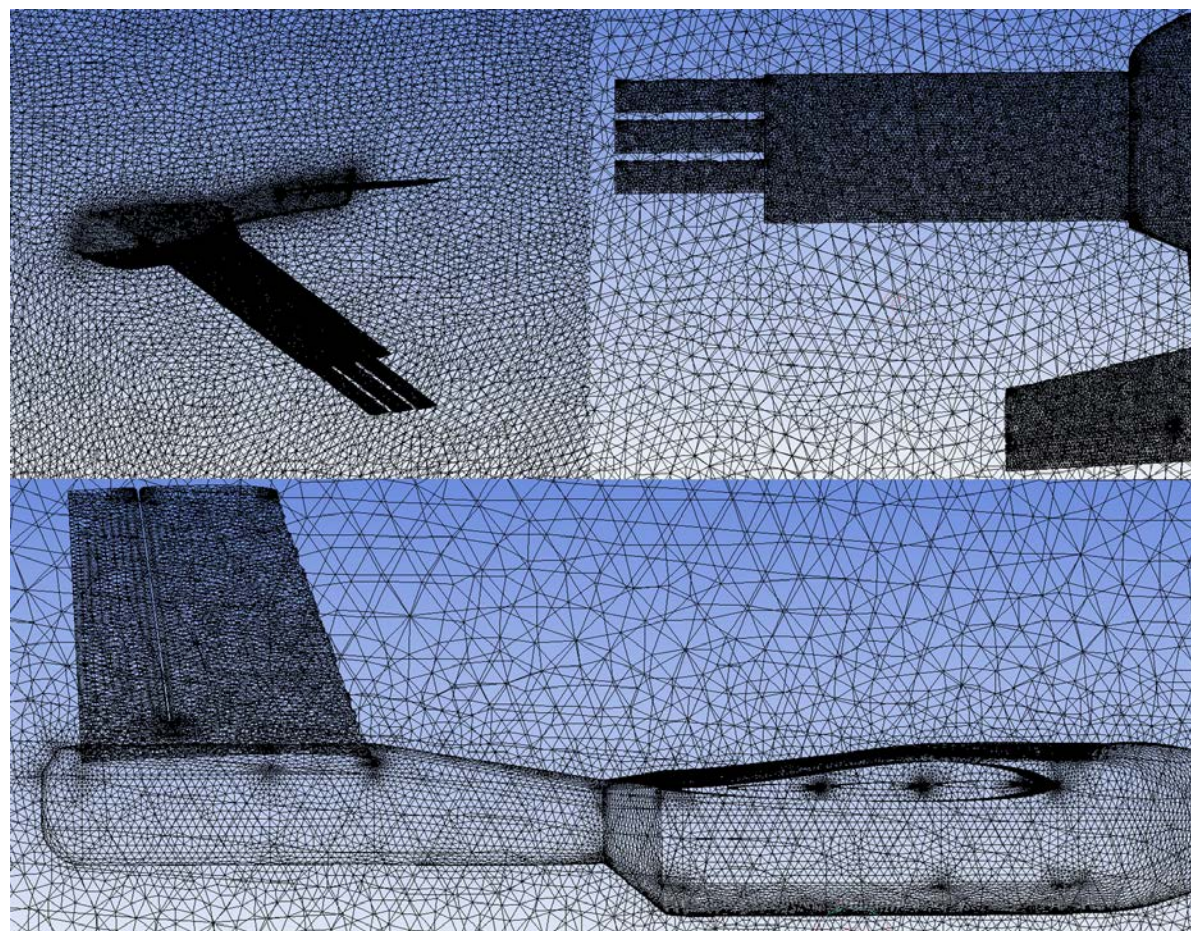
ANSYS-Fluent.



Mesh characteristics

Mesh characteristics:

- 3D mesh.
- Unstructured mesh.
- Tetrahedral cells.
- ~ 5 millions of elements.
- Sizing of 0.002 m.



2.0 NUMERICAL ANALYSIS

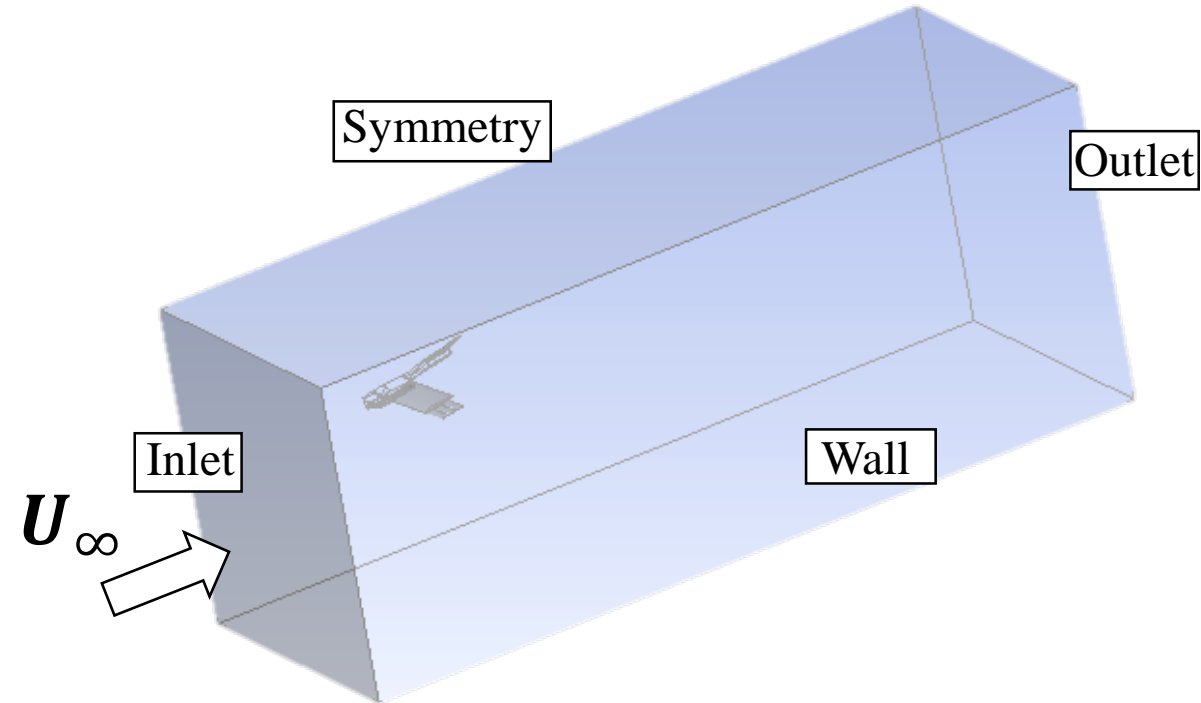
ANSYS-Fluent.



Solver characteristics

Boundary conditions

- Inlet velocity: 16 m/s.
- Outlet pressure.
- Wall condition.
- Symmetry condition.



Turbulence model: $k - w$ model



1.0 INTRODUCTION

2.0 NUMERICAL ANALYSIS

3.0 EXPERIMENTAL SET-UP

3.1 Low-Speed Wind Tunnel

3.2 Manufacturing process

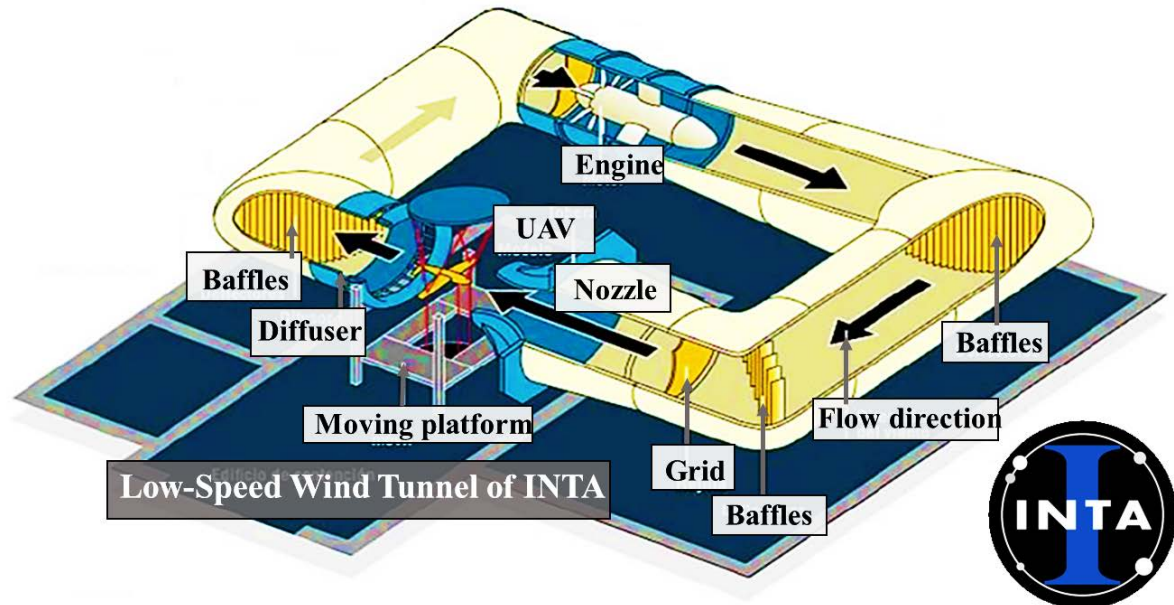
3.3 Experimental tests

4.0 RESULTS

5.0 SUMMARY AND CONCLUSIONS

3.0 EXPERIMENTAL SET-UP

Low-Speed Wind Tunnel of INTA.



CHARACTERISTICS:

- Wind tunnel with closed circuit.
- Elliptical test section of 2x3 m².
- Maximum air velocity of 60 m/s.
- Turbulence intensity lower than 0.5%.
- Moving platform.
- Streamlined leading and trailing edge.
- DC engine of 450 kW (working at 420 V).

3.0 EXPERIMENTAL SET-UP

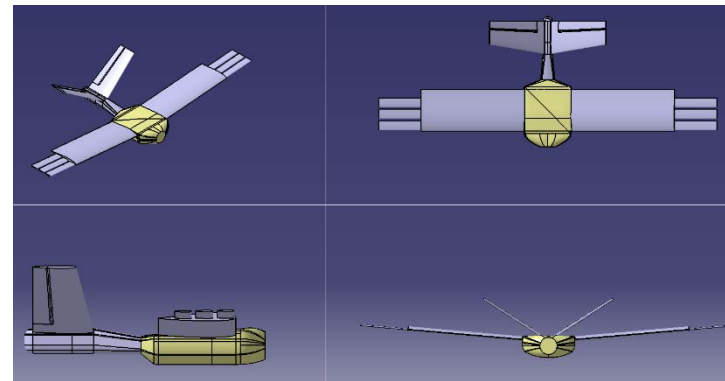
Manufacturing process.

- ❑ 3D printing technique:
 - Reduces time and cost compared with traditional methods.
 - High resolution in complex geometries.

- ❑ Additive material: PLA.

- ❑ BCN+ 3D printing machine: Low-cost machine. Price ~ 4.000-5.000€

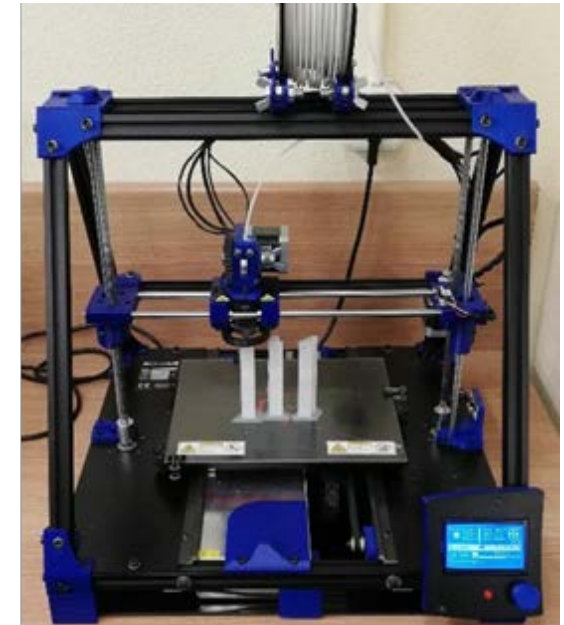
UAV views in CATIA



PLA properties

Property	Value
Technical Name	Polylactic Acid (PLA)
Melt Temperature	157 - 170 °C
Typical Injection Molding Temperature	178 - 240 °C
Tensile Strength	61 - 66 MPa
Flexural Strength	48 - 110 MPa
Specific Gravity	1.24
Shrink Rate	0.37 - 0.41 %

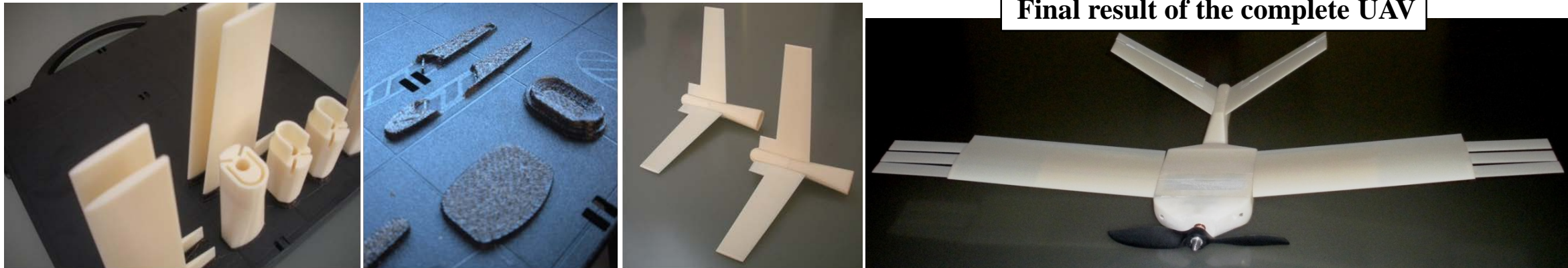
Low-cost BCN+ 3D printing machine



3.0 EXPERIMENTAL SET-UP

Manufacturing process.

Full-scale model (1:1)
Less than a day (~16 hours)
Price of the complete UAV ~ 100€



Final result of the complete UAV

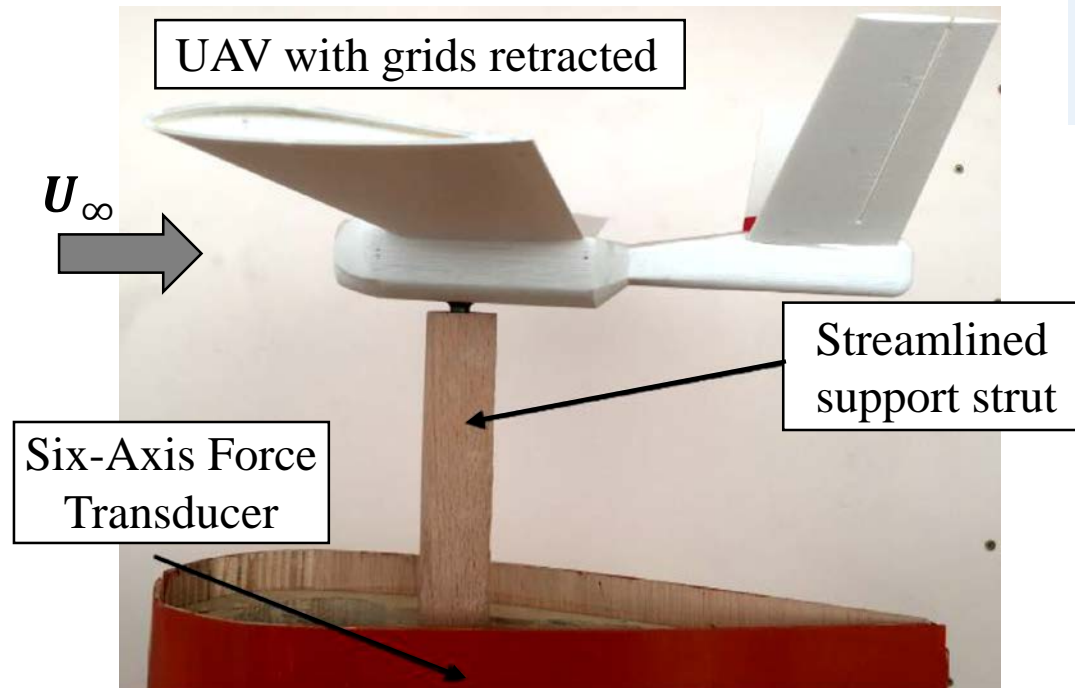
- ❑ All components are manufactured in **vertical direction**, layer-by-layer.
- ❑ The model surface is polished to reduce the roughness
- ❑ This finishing process is enhanced by spraying a light coat of painting.



Avoid boundary layer change.

3.0 EXPERIMENTAL SET-UP

Experimental tests.



Conditions:

- Two UAV configurations: **Retracted grids and Extended grids.**
 - Several angles of attack: -10° to 25°
 - Airflow velocity of 16 m/s ($Re = 9.2 \times 10^4$).
 - Complete UAV
-
- Streamlined support strut: to reduce the flow perturbations.
 - Six-Axis Force Transducer: to measure the lift and drag forces.
 - ATI Mini40.
 - Labview software: to store the data acquisition.
 - Recording time: 4 minutes.
 - Sampling time: 1993 Hz.
 - ATI Mini40 transducer was just placed on the center of gravity of the UAV model.



1.0 INTRODUCTION

2.0 NUMERICAL ANALYSIS

3.0 EXPERIMENTAL SET-UP

3.1 Low-Speed Wind Tunnel

3.2 Manufacturing process

3.3 Experimental tests

4.0 RESULTS

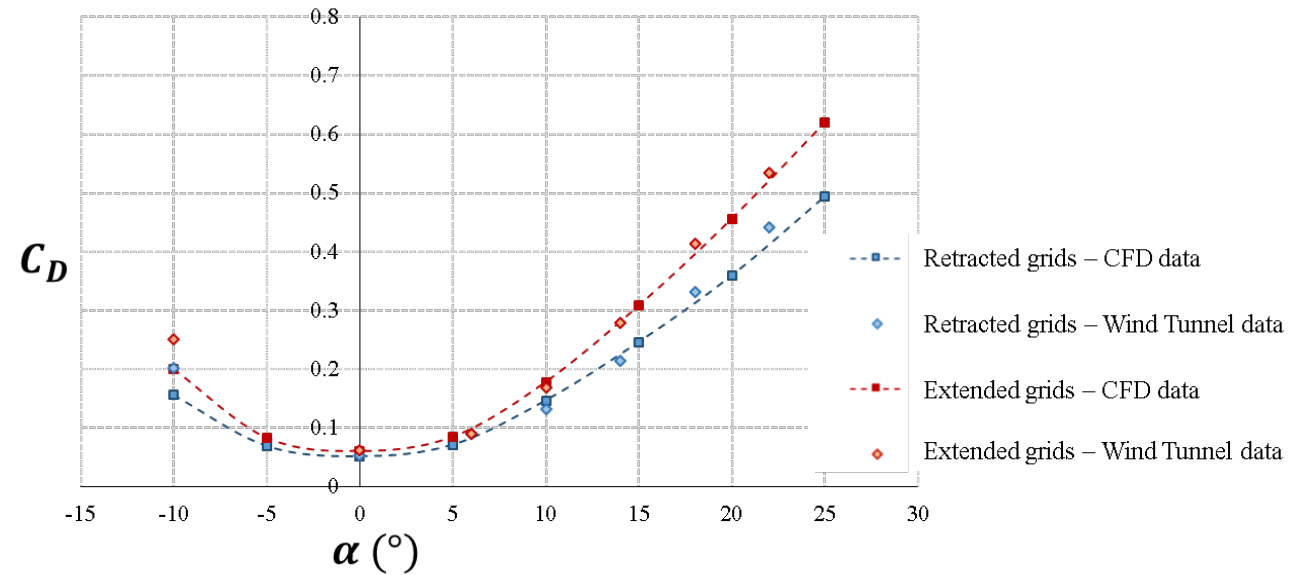
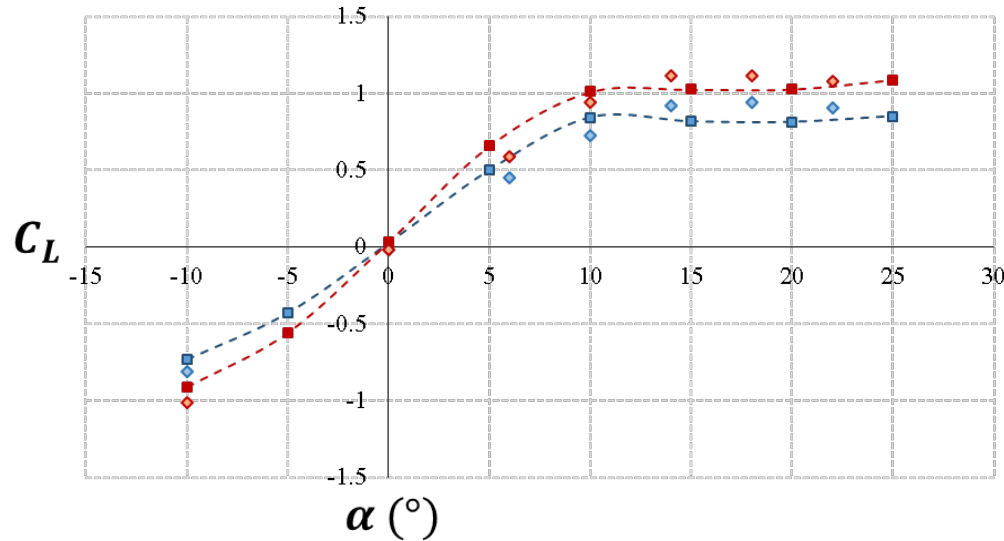
5.0 SUMMARY AND CONCLUSIONS

4.0 RESULTS

Lift and drag coefficients.

$$\text{Lift coefficient } C_L = \frac{L}{\frac{1}{2}\rho V^2 S_{ref}};$$

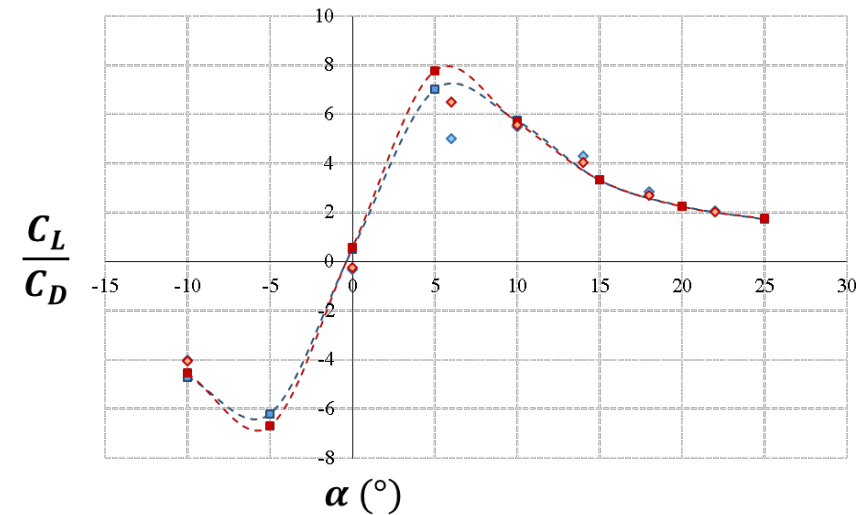
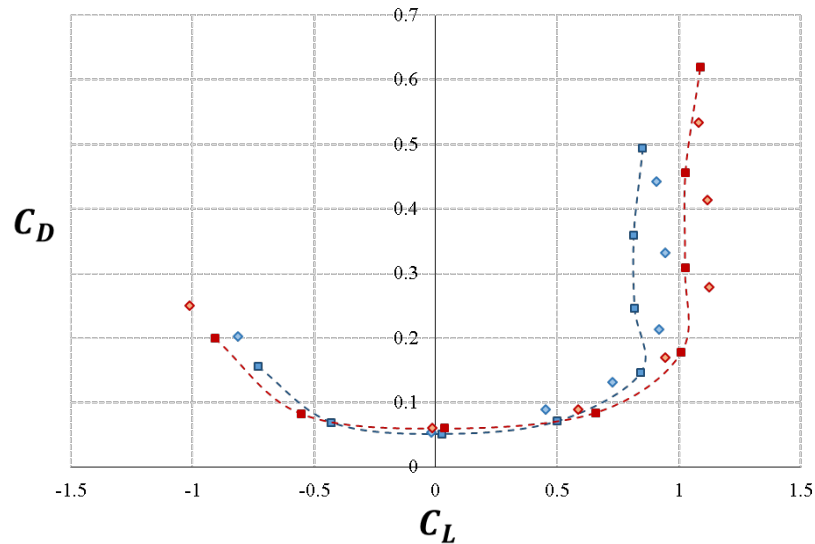
$$\text{Drag coefficient } C_D = \frac{D}{\frac{1}{2}\rho V^2 S_{ref}}$$



- ❑ $\alpha > 0^\circ$: the lift force with extended grids is higher than retracted grids.
- ❑ $-10^\circ < \alpha < 25^\circ$: the drag force with extended grids is higher than retracted grids.
- ❑ $-5^\circ < \alpha < 5^\circ$: the increase in drag with extended grids is around 15% higher than retracted grids.
- ❑ **Relative error in drag values between numerical and experimental data of 5% or less for low angles of attack.**

4.0 RESULTS

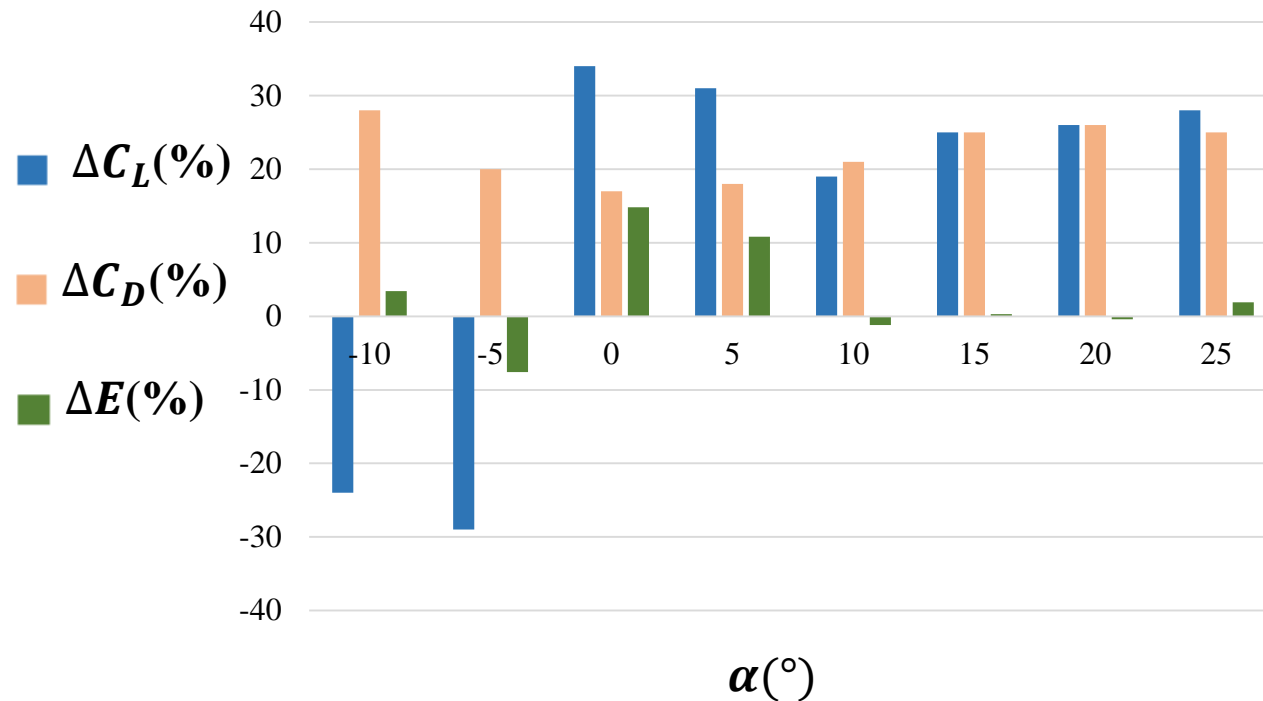
Polar drag and aerodynamic efficiency.



- ❑ Polar drag: for a constant drag force, there is more lift generated by the extended grid configuration.
- ❑ For $\alpha = 5^\circ$: maximum aerodynamic efficiency for both configurations.
- ❑ For $\alpha > 5^\circ$: same aerodynamic efficiency for both configurations.

4.0 RESULTS

Percentage variation in aerodynamic performance of the UAV with extended grids – retracted grids (%).



ΔC_L (%): percentage variation in lift coefficient extended – retracted grids.

ΔC_D (%): percentage variation in drag coefficient extended – retracted grids.

ΔE (%): percentage variation in aerodynamic efficiency extended retracted grids.

For cruise and loiter phases:

The extended grid configuration presents a higher aerodynamic efficiency than the retracted grid configuration (~10%). The grids will be extended.

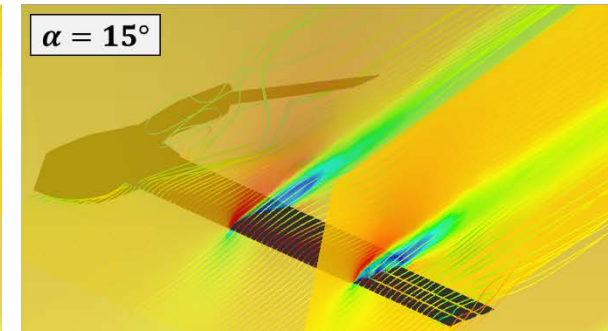
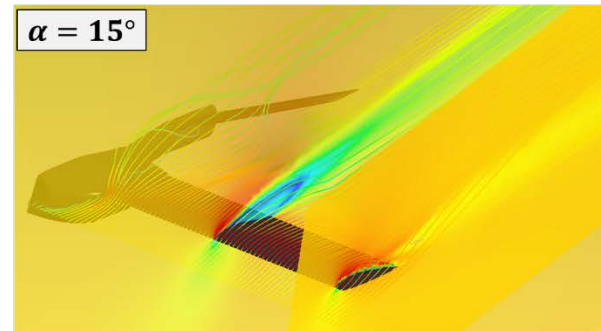
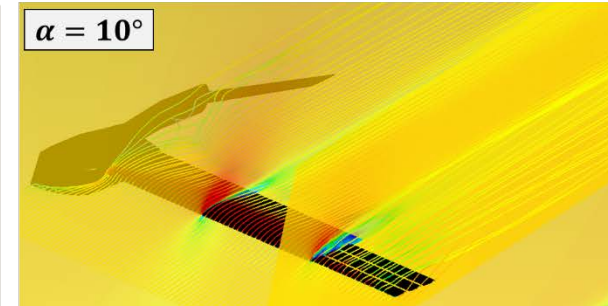
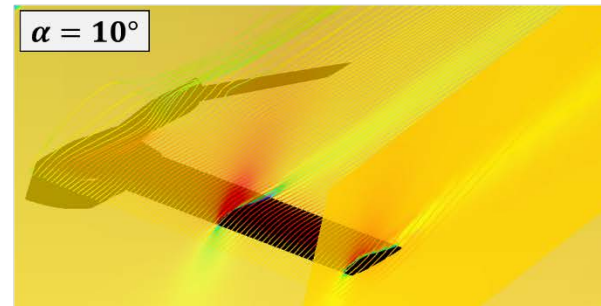
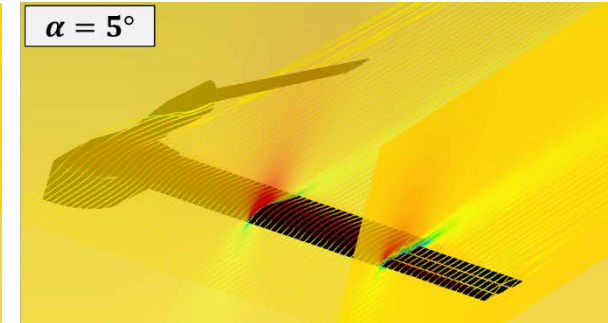
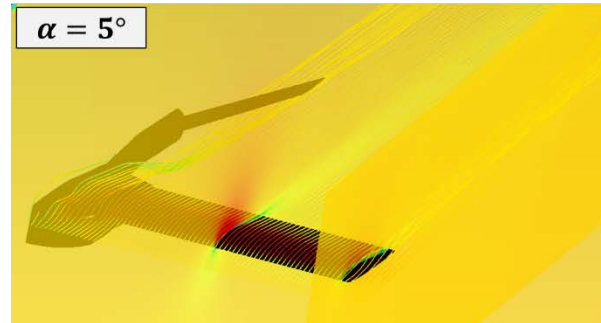
For landing and take-off phases:

The grids should be retracted.

4.0 RESULTS

Flow visualization.

- ❑ $\alpha = 5^\circ$: flow is completely attached in both configurations.
- ❑ $\alpha = 10^\circ$: flow is attached to the wing. Flow detachment around the grids.
- ❑ $\alpha = 15^\circ$: recirculation bubble over the wing which deteriorates the aerodynamic performances in both configurations.





1.0 INTRODUCTION

2.0 NUMERICAL ANALYSIS

3.0 EXPERIMENTAL SET-UP

3.1 Low-Speed Wind Tunnel

3.2 Manufacturing process

3.3 Experimental tests

4.0 RESULTS

5.0 SUMMARY AND CONCLUSIONS

5.0 SUMMARY AND CONCLUSIONS

Summary.

- A numerical and experimental analysis of a biomimetic UAV with grids that simulates the primary feathers of birds has been carried out.
- The aerodynamic performances have been obtained by using CFD simulations and wind tunnel measurements.

5.0 SUMMARY AND CONCLUSIONS

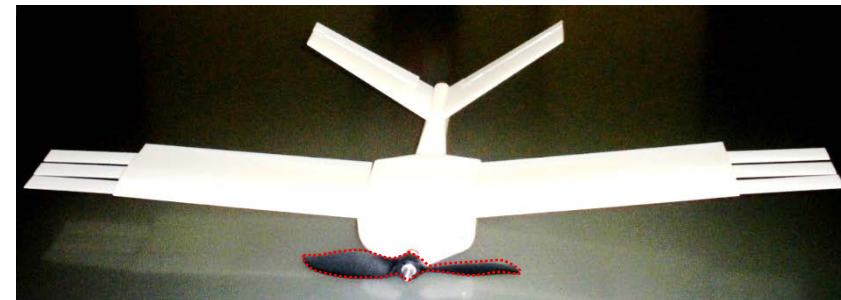
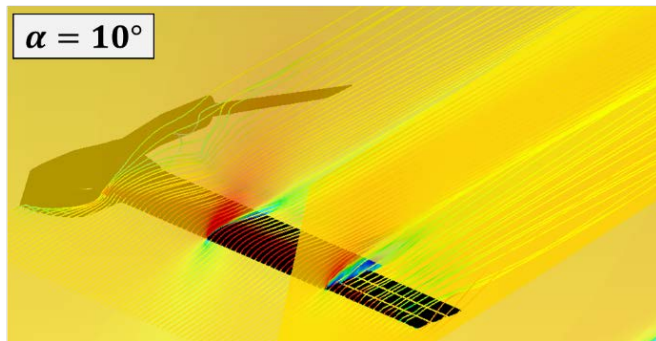
Conclusions.

- For cruise and loiter flight phases the grids should be extended since the aerodynamic efficiency is 10% higher, while for landing and take-off maneuvers they should be retracted.
- The deployment in cruise and loiter phases will increase the lift of the vehicle, allowing an increase in range or autonomy.
- Numerical and experimental data have shown good agreement with a relative error in drag values of 5 % or less for low angles of attack ($-5^\circ \leq \alpha \leq 5^\circ$).

5.0 SUMMARY AND CONCLUSIONS

Next Steps.

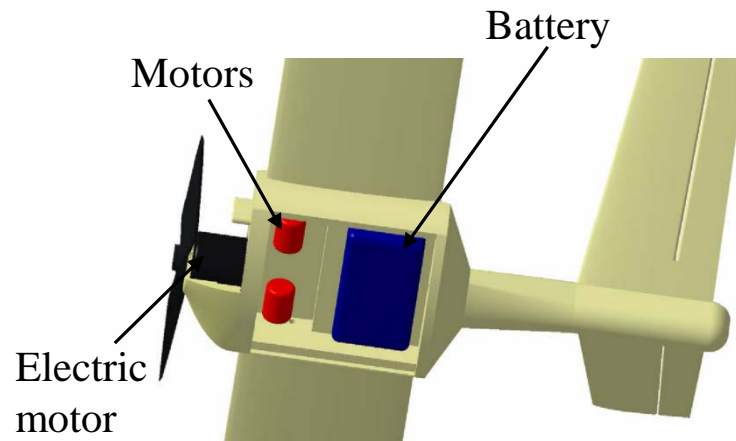
- 1st phase:** CFD simulations – wind tunnel testing – aerodynamics.
- 2nd phase:** Interaction traction propeller on aerodynamics – numerical and wind tunnel.



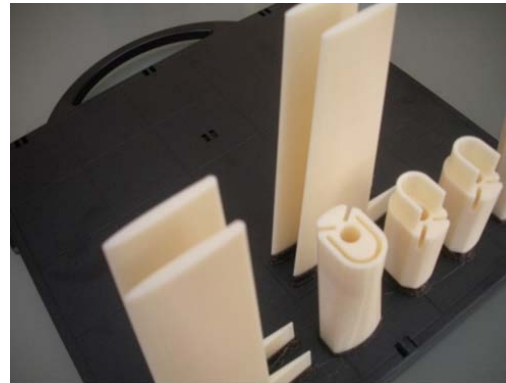
5.0 SUMMARY AND CONCLUSIONS

Next Steps.

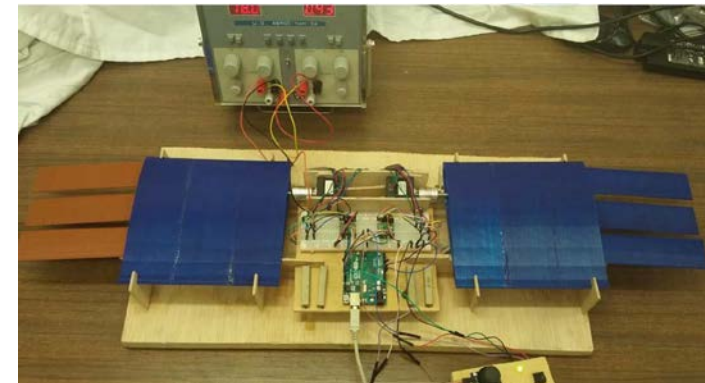
- ❑ **3rd phase:** Fabrication of the real demonstrator with flight test instrumentation.



Real demonstrator design



3D manufacturing process



Prototype and control system

- ❑ **4th phase:** Flight testing (pressure sensors, accelerometers, flight data recorders).

THANK YOU FOR YOUR ATTENTION
QUESTIONS?



Flight Testing of Unmanned Aerial Systems (UAS) Segovia, Spain, 12-13 May 2022



Numerical and Experimental Study of a Biomimetic UAV with Grids

SCI-328 Symposium

Components	Description	Weight (g)
Structure	For a vehicle with a wingspan of 0,72 m	400
Wing-grid mechanism	Deployment system for wing grids. Motors and actuators	40
Motor	Electric motor driving propeller for 0.7 kg vehicle	60
Battery	LiPo battery for the electric motor	130
Electronics components and microsensors	UAV control electronics and microsensors	30
Payload	Lightweight micro camera	10
Preliminary weight estimation		670